Progress In Electromagnetics Research C, Vol. 135, 55–67, 2023

Dual-Band 4 × 4 Hexagonal SRR MIMO Antenna with Port Excitation-Controlled Gain and Directivity for WLAN/WiMAX Applications

Puneet Sehgal[1, 2] and Kamlesh Patel[2, *]

Abstract—This paper presents the total gain and directivity control with port excitation in a 4 × 4 hexagonal split-ring resonator (H-SRR) MIMO antenna for dual-band operation in 2.4/5.2 GHz bands. The MIMO antenna shows more than 15 dB isolation between antenna elements placed orthogonally, and a spacing was introduced between them to achieve higher isolation in the first proposed design, then, a Z-structure of specific dimensions was inserted to further improve the isolation between antenna elements. The simulated and measured return losses and transmission coefficients confirmed improved impedance bandwidth and isolation performances. The gain, axial ratio, and radiation pattern performances of the 4 × 4 H-SRR MIMO antenna are studied by exciting different port combinations of the proposed antenna. A wide range of gain and axial ratio variations are observed on exciting single, dual, triple, and quad-ports of the proposed MIMO antenna and discussed using the radiation patterns. Also, various MIMO parameters, ECC < 0.04, TARC < −10 dB, MEG < −6 dB, DG < 10 dB, and CCL < 0.4 bits per second per Hz, are found in the 2.4/5.2 GHz bands, which confirms the applicability of proposed H-SRR MIMO antenna with polarization diversity.

1. INTRODUCTION

With the advancement of wireless technology, the demand for high bandwidth arose, and hence the channel capacity of the communication channel should be high to accommodate more signals of high-frequency use for several small devices [1], thus reducing the channel capacity loss (CCL) results in the efficient transmission of a signal from transmitter to receiver. So, to meet the higher rate demanding a wide frequency band at a very low power level, ultra-wideband (UWB) technology is required to grow faster for the consumers at an effective lower cost [2]. Such research requirement has attracted the interest of researchers from academia and industries after the authorization to use the unlicensed applications of the 3.1–10.6 GHz band by the Federal Communication Commission (FCC) [3]. The main disadvantages of a UWB system are multipath fading signal due to reflection and diffraction between the receiver and transmitter [4], and poor reliability that deteriorates the performance of the system [5]. In addition to solving these issues, multiple-input-multiple-output (MIMO) systems provide a more practical and appropriate solution without any extra burden of bandwidth and power [6, 7] as in such systems, multiple antennas are used to transmit and receive the signals, and a method is analyzed to estimate the channel capacity in MIMO fading systems in the past [8].

Many UWB MIMO antennas have been reported earlier for the literature review of various UWB systems [9, 10]. It has been observed in the past that UWB technology faces a strong issue of electromagnetic signal interference with our existing narrow band communication system such as the IEEE wireless local area network in the 5.2 GHz range in which split ring resonator (SRR) structures

Received 6 March 2023, Accepted 8 July 2023, Scheduled 24 July 2023

* Corresponding author: Kamlesh Patel (kpatel@south.du.ac.in).

[1] Atma Ram Sanatan Dharma College, University of Delhi, Dhaula Kuan, New Delhi 110021, India. [2] Department of Electronic Science, University of Delhi South Campus, New Delhi, India.

are proposed to achieve band rejection [11]. However, SRR structures help in increasing the bandwidth of antenna-like application in quad-band operation [12], thus SRR structures find their utility to cover WLAN/WiMAX/5G bands for a wide application range in 2.4/5.2/5.8 GHz bands. Hence, the purpose of eliminating the band rejection is difficult to achieve with proper band notch characteristics as reported for UWB antennas [13], so it is a challenging task to balance between the two. Normally in a typical MIMO antenna, the distance between two antennas should be kept at a minimum of $\lambda/2$ for an acceptable limit of isolation between the antennas, and the better the isolation is, the better the gain performance of the antenna will be, producing circular polarization in the antenna. Hence to achieve a compact MIMO antenna, the distance between two antenna elements is reduced with orthogonal placement which further decreases the isolation between the antenna elements and hence results in a low value of the envelope correlation coefficient (ECC) and CCL. In the past, various values of diversity parameters of a 4-port MIMO antenna were reported as ECC of 0.005 and CCL of 0.3 bits per second per Hz [18, 19], ECC of 0.0022 and CCL of 0.30 bits per second per Hz [14], ECC of 0.4 and CCL less than 0.4 bits per second per Hz, CCL of 0.3 bits per second per Hz and ECC of 0.005 [20], ECC of 0.1 while CCL < 1 for 3 to 5 GHz frequency range and CCL < 0.1 for frequency more than 5 GHz reported earlier [21]. Thus, it can be observed that the right value of ECC and CCL plays a pivotal role in the better performance of the MIMO antenna to radiate with maximum gain and minimum losses in the form of fading of the signals during the communication process [22].

In this paper, a hexagonal split ring resonator (H-SRR) with coplanar waveguide transmission (CPW) feed element based 4×4 MIMO antenna is proposed as a compact dual-band monopole antenna with more than 15 dB isolation between antenna elements placed orthogonally (design 1). Then, a Z-shaped structure of specific dimensions is inserted to improve isolation to better than 20 dB at 2.4/5.2 GHz bands and named as the second design (design 2). Both designs are simulated in ANSYS High-Frequency Structure Simulator (HFSS) software, and then design 2 is fabricated for measurement with R&S handheld VNA ZVH8. The gain and axial ratio values are studied very less concerning the different port excitations in MIMO antennas, although the same is required to assess the effectiveness of pattern and polarization diversities of MIMO antenna. This analysis is made in the present work by exciting different ports individually as such information is useful for enhanced channel capacity, covering a large range of polarization-based applications.

2. DESIGN OF HEXAGONAL SRR MIMO ANTENNA

The proposed antenna consists of four orthogonally placed and CPW-fed H-SRR antenna elements as shown in Figure 1, where design 1 is MIMO antenna without Z-structure, and design 2 is MIMO

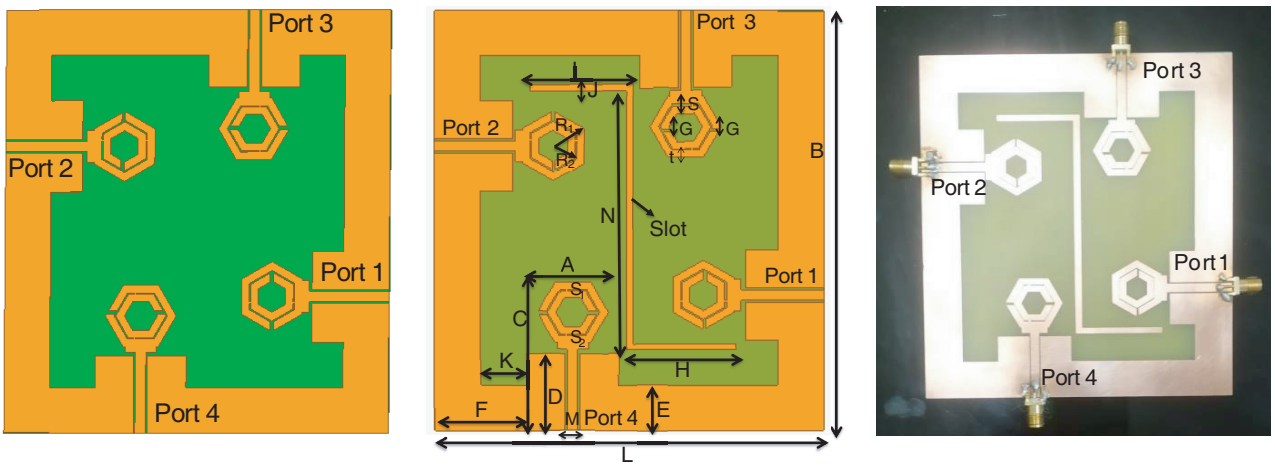

(a) (b) (c)

Figure 1. (a) Schematic layout of a proposed 4×4 H-SRR MIMO antenna without Z-structure (design 1). (b) MIMO antenna with Z-structure (design 2). (c) Fabricated prototype of MIMO antenna (design 2).

antenna with Z-structure, with the fabricated antenna of design 2 (as shown in Figure 1(c)). Each antenna element is of size $43 \times 26 \times 1.5\,\text{mm}^3$ and made by two SRRs of outer radius $R_1 = 7.5\,\text{mm}$ and inner radius $R_2 = 5.5\,\text{mm}$. The substrate used is FR-4 with the relative permittivity $\varepsilon_r = 4.4$, height $h = 1.5\,\text{mm}$, and $35\,\mu\text{m}$ thick copper layer. To obtain better impedance matching and isolation between the antenna elements, a Z-structure is inserted in between as shown in Figure 1(b). The size of the 4×4 H-SRR MIMO antenna is optimized to $121 \times 110 \times 1.5\,\text{mm}^3$, and other dimensions of the final MIMO antenna of design 2 are shown in Table 1.

Table 1. Dimensions of the antenna element and proposed MIMO antenna (design 2).

Various parameters	**Values (in mm)**
Length of the antenna (L)	121
The breadth of the antenna (B)	110
$A = F$	26
Length of the ground planes (C)	43
D	22
$E = K$	13
N	73
$H = I$	29
J	2
Metallic loadings ($S_1 = S_2$)	$1.5 \times 0.5\,\text{mm}^2$
The gap within both rings ($G_1 = G_2 = G$)	1
S	0.5
t	2.5
Width of the center CPW line (M)	3

3. PERFORMANCE OF THE 4×4 H-SRR MIMO ANTENNA

3.1. Simulated and Measured Return Loss (S_{Ii}) and Transmission Coefficients (S_{ij})

The return loss and other transmission coefficients are measured using R&S handheld VNA ZVH8 in the anechoic chamber as shown in Figure 2(a). The simulated return loss (S_{ii}, where $i = 1, 2, 3, 4$) of proposed MIMO antenna with design 1 and design 2 along with measured results of the fabricated MIMO antenna design 2 are presented in Figure 2(b). Other simulated and measured transmission coefficients for design 1 and design 2 at 2.4/5.2 GHz frequencies are shown in Table 2.

Table 2 shows that design 2 gives better matching and isolation among the four radiating antennas due to the insertion of the Z-structure. A slight shift towards higher frequency is observed in the S-

Table 2. Various transmission coefficients of the proposed MIMO antenna.

S-parameters	**design 1 (Simulated) (2.4/5.2 GHz)**	**design 2 (Simulated) (2.4/5.2 GHz)**	**design 2 (Measured (2.4/5.2 GHz)**
S_{11}	$-8.83/-21.35\,\text{dB}$	$-10.04/-15.61\,\text{dB}$	$-16.70/-14.06\,\text{dB}$
Isolation (S_{21})	$-17.44/-35.20\,\text{dB}$	$-16.73/-32.44\,\text{dB}$	$-0.60/-16.36\,\text{dB}$
S_{31}	$-19.73/-23.16\,\text{dB}$	$-24.84/-29.58\,\text{dB}$	$-10.00/-28.60\,\text{dB}$
S_{41}	$-15.48/-32.75\,\text{dB}$	$-13.33/-31.33\,\text{dB}$	$-10.00/-34.64\,\text{dB}$
Angle S_{21}	$96.58°/89.48°$	$76.14°/-177.41°$	$-313.13°/-282.30°$

(a)

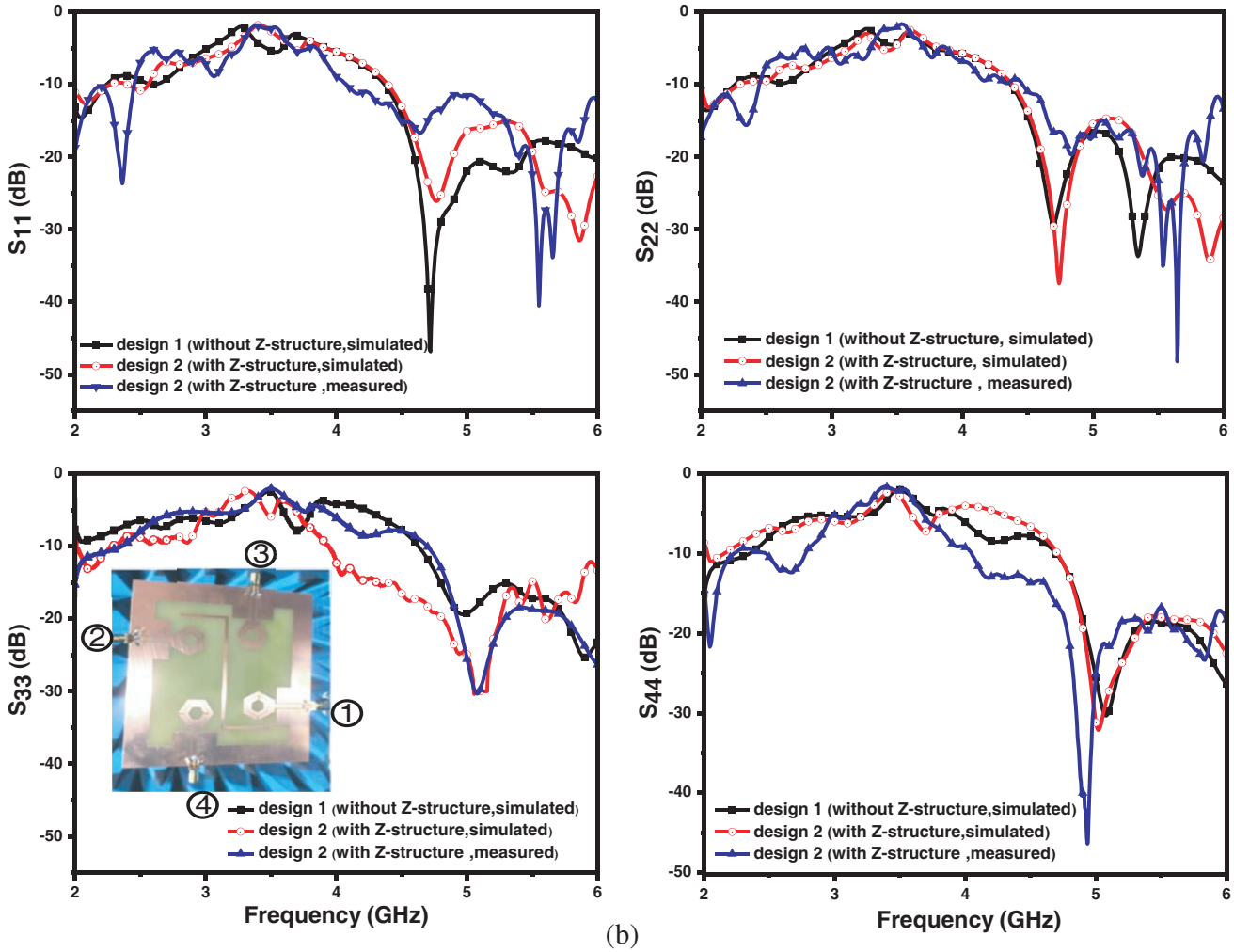
S11 (dB)
S22 (dB)
S33 (dB)
S44 (dB)
Frequency (GHz)
design 1 (without Z-structure,simulated)
design 2 (with Z-structure,simulated)
design 2 (with Z-structure ,measured)
design 1 (without Z-structure, simulated)
design 2 (with Z-structure, simulated)
design 2 (with Z-structure , measured)
①
②
③
④

(b)

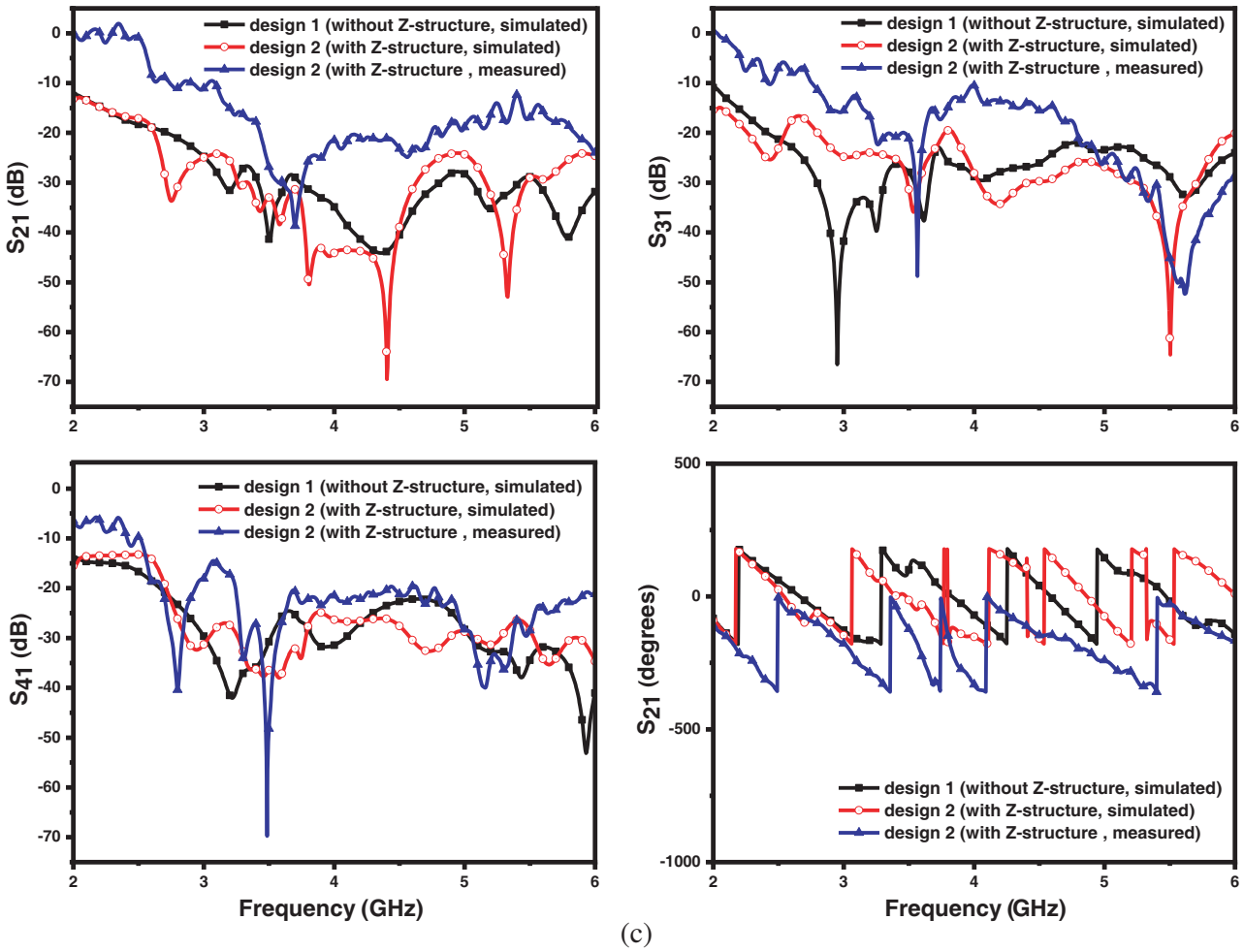

Figure 2. S-parameters of 4×4 H-SRR MIMO antenna. (a) Measurement set up for S-parameter measurements using R&S VNA model ZVH8 in the anechoic chamber. (b) S_{11}, S_{22}, S_{33}, and S_{44} responses and (c) S_{12}, S_{13}, S_{14} and angle of S_{21} responses.

parameters responses. The simulated impedance bandwidth (IBW) is found to be 68.46% for design 1 and 75.96% for design 2 while the measured IBW of design 2 is 76.92%, and an improvement of 1.26% is noted in IBW due to the Z-structure at 2.4 GHz. Hence, it is verified that the proposed design provides good isolation and high bandwidth for WLAN/WiMAX bands applications.

3.2. Gain and Radiation Pattern Performance

To study the gain and radiation pattern performances of the proposed MIMO antenna (design 2), four cases are considered based on port excitation, (i) case 1 when only Port 1 is excited, (ii) case 2 when Port 1 and Port 3 are excited, (iii) case 3 when three ports, i.e., Ports 1, Port 2, and Port 3, are excited together, and in (iv) case 4, where four ports, i.e., Port 1, Port 2, Port 3, and Port 4, are excited together. In Figure 3(a), the simulated gain response shows that for case 1, the gain is varied from -0.15 dB to 5.97 dB in the 2 to 6 GHz range, whereas for case 2 its range is -0.02 dB to 6.22 dB, and the gain is decreased to the range -0.0071 to 3.65 dB. When Port 4 is excited in addition, i.e., case 4, the gain is deeply reduced to $-31.96/-18.64$ dB at 2.4/5.2 GHz. This indicates that due to the pattern diversity, the antenna gain varies in a wide range for case 1 to case 2 in the proposed MIMO antenna. To confirm this, the 3D radiation pattern is studied and shown in Figure 3 for all combinations of the port excitation from cases 1 to 4. As in Figure 4, the proposed antenna fulfills the requirements

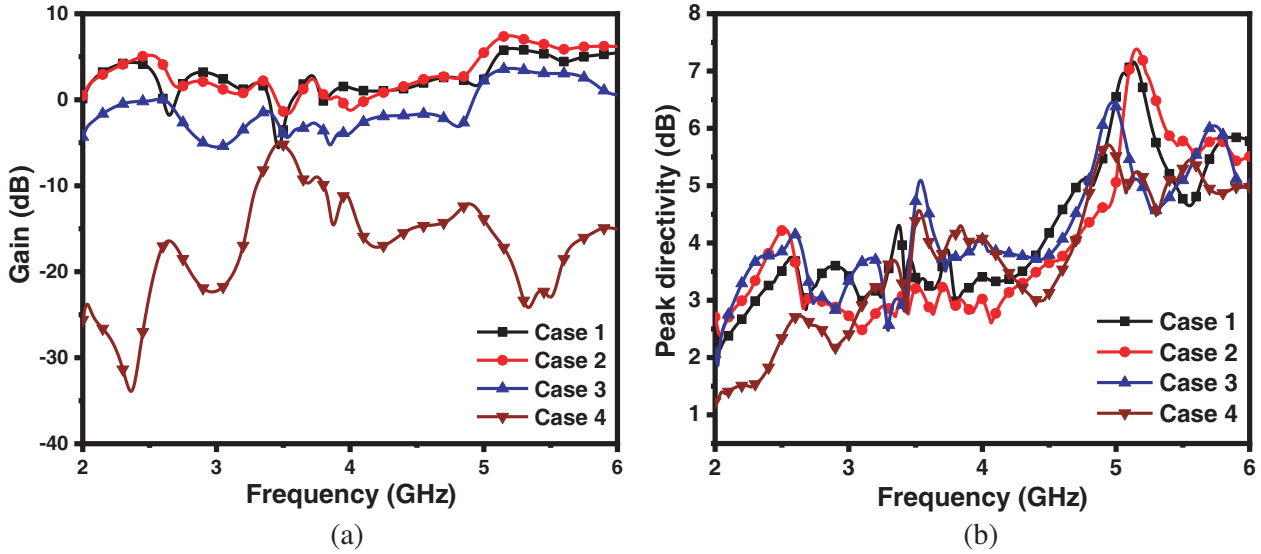

Figure 3. (a) Simulated gain, and (b) Simulated peak directivity of the 4×4 H-SRR MIMO antenna.

of orthogonality on a single or more port excitation. The directions of maximum gain vary based on the position of the antenna element and operating frequency in addition to beamwidth. A narrower beamwidth is observed at 5.2 GHz than at 2.4 GHz frequency for all cases.

The radiation patterns of two orthogonally placed antenna elements added and higher gain values are obtained for case 2 as shown in Figures 4(i)–(j). In Figures 4(k)–(o) for cases 3 to 4, the multi-beam formation led to the reduction in the gain values due to the cross-polarization of radiation patterns arising from the orthogonally placed individual antenna elements. With all four ports being excited simultaneously, i.e., case 4, the antenna with high negative gain emerges and finds its application in the field of lower gain RFID antenna where the low gain antennas of smaller size are preferred as compared to high gain antennas [15]. Depending upon the application of the RFID tag, the low gain antenna is useful to read by the reader in the lower range.

It can be observed that out of the four studied cases, the port excitation with orthogonal ports of the radiating antenna elements, i.e., case 2 (Port 1 and Port 3 excitation) is the best choice for an enhanced gain of 4.77/7.44 dB and peak directivity of 5.82/8.57 dB at 2.4/5.2 GHz as shown in Figure 3(b), respectively. In addition, a wide beamwidth of 49.36°/31.37° is observed for H-plane at 2.4/5.2 GHz bands. Thus, a narrower beamwidth and higher gain direct a good signal strength in a particular direction of the antenna. Hence, the gain of the proposed MIMO antenna can be controlled from 5 dB to −31 dB by exciting ports simultaneously or individually in various port excitation combinations as discussed above without affecting the radiation pattern much as similar beamwidth is obtained at 2.4/5.2 GHz bands, respectively as summarized in Table 3. Figure 5 presents the simulated H and E-plane radiation patterns of the designed antenna at 2.4 and 5.2 GHz frequencies, respectively. It should be noted that the patterns at operating frequency bands are omnidirectional in the E-plane and dipole-like in H-plane except in the notched band at 5.2 GHz. It can also be observed that at higher frequency bands, radiation lobes are split due to higher-order mode propagation and due to multi-antenna radiations.

Figure 6 shows the axial ratio obtained for the four cases of port excitation of the proposed MIMO antenna, and it confirms that linear or circular polarization can be obtained in different frequency bands by exciting various ports. The axial ratio in Figure 6(a) for case 1, when a single port 1 is excited, shows circular polarization in the 3.47–3.485 GHz band, while it is in the 3.485–3.51 GHz band for case 2. The circular polarization shifts to the lower range of frequencies of 2.645–2.675 GHz in case 3 and to the higher band of 5.49–5.54 GHz for case 4. For remaining frequency bands, it shows linear polarization. Thus, such an antenna can produce a linear or circular polarization by controlling the feeding at single or multi-ports in both lower and upper ranges of frequencies.

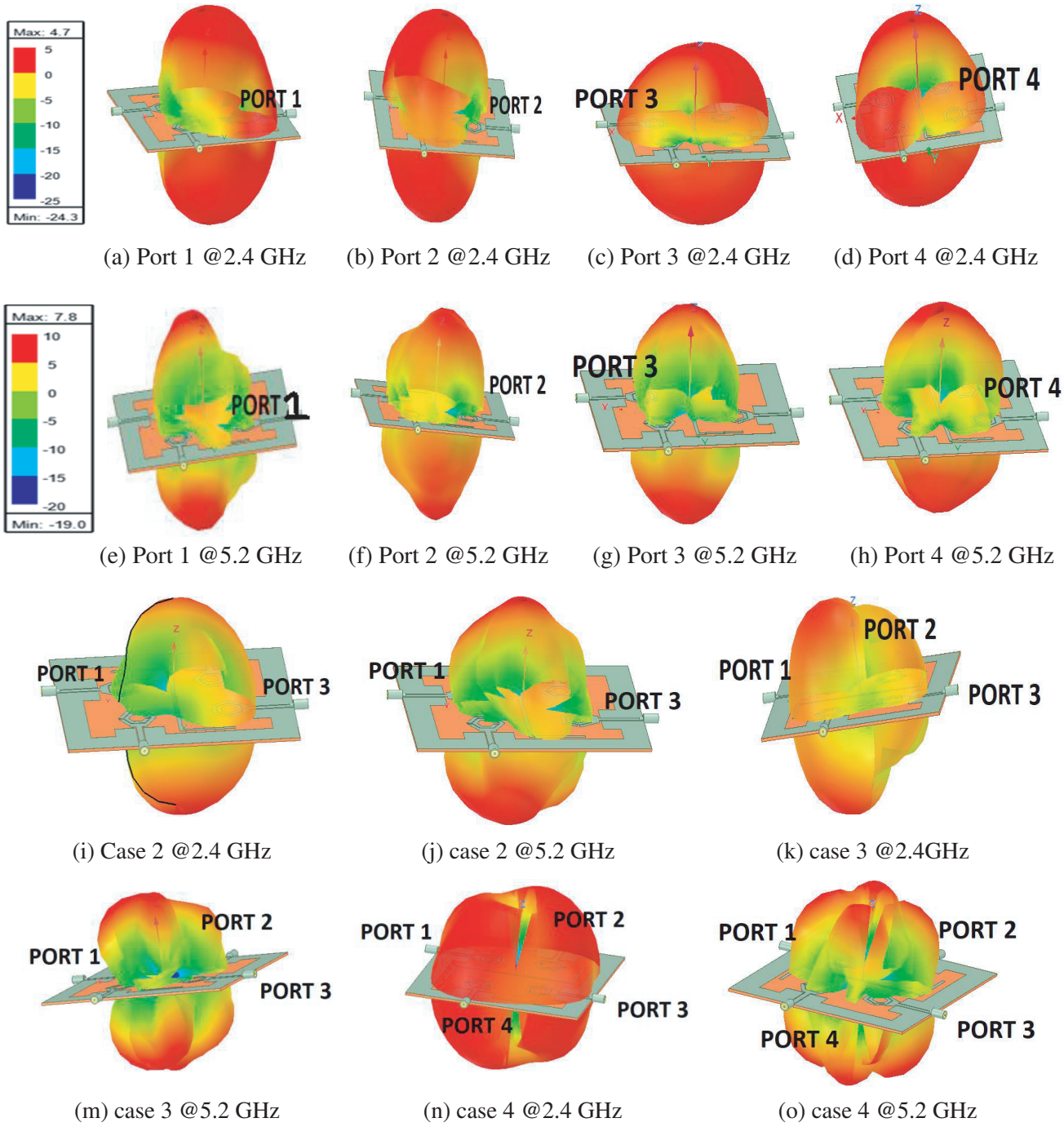

(a) Port 1 @2.4 GHz (b) Port 2 @2.4 GHz (c) Port 3 @2.4 GHz (d) Port 4 @2.4 GHz

(e) Port 1 @5.2 GHz (f) Port 2 @5.2 GHz (g) Port 3 @5.2 GHz (h) Port 4 @5.2 GHz

(i) Case 2 @2.4 GHz (j) case 2 @5.2 GHz (k) case 3 @2.4GHz

(m) case 3 @5.2 GHz (n) case 4 @2.4 GHz (o) case 4 @5.2 GHz

Figure 4. 3D polar plots of 4×4 H-SRR MIMO antenna (design 2) for (a)–(h) case 1, (i)–(j) case 2, (k)–(m) case 3 and (n)–(o) case 4 at 2.4/5.2 GHz.

4. DIVERSITY CHARACTERISTICS OF THE PROPOSED 4×4 H-SRR MIMO ANTENNA

Next, the diversity performance of the proposed MIMO antenna is studied by evaluating the Envelope Correlation Coefficient (ECC), Total Active Reflection Coefficient (TARC), Mean Effective Gain (MEG), Diversity Gain (DG), and CCL. For the proposed MIMO antenna, the ECC between two antenna elements, i.e., antenna i and antenna j can be obtained from their far-field radiation patterns using

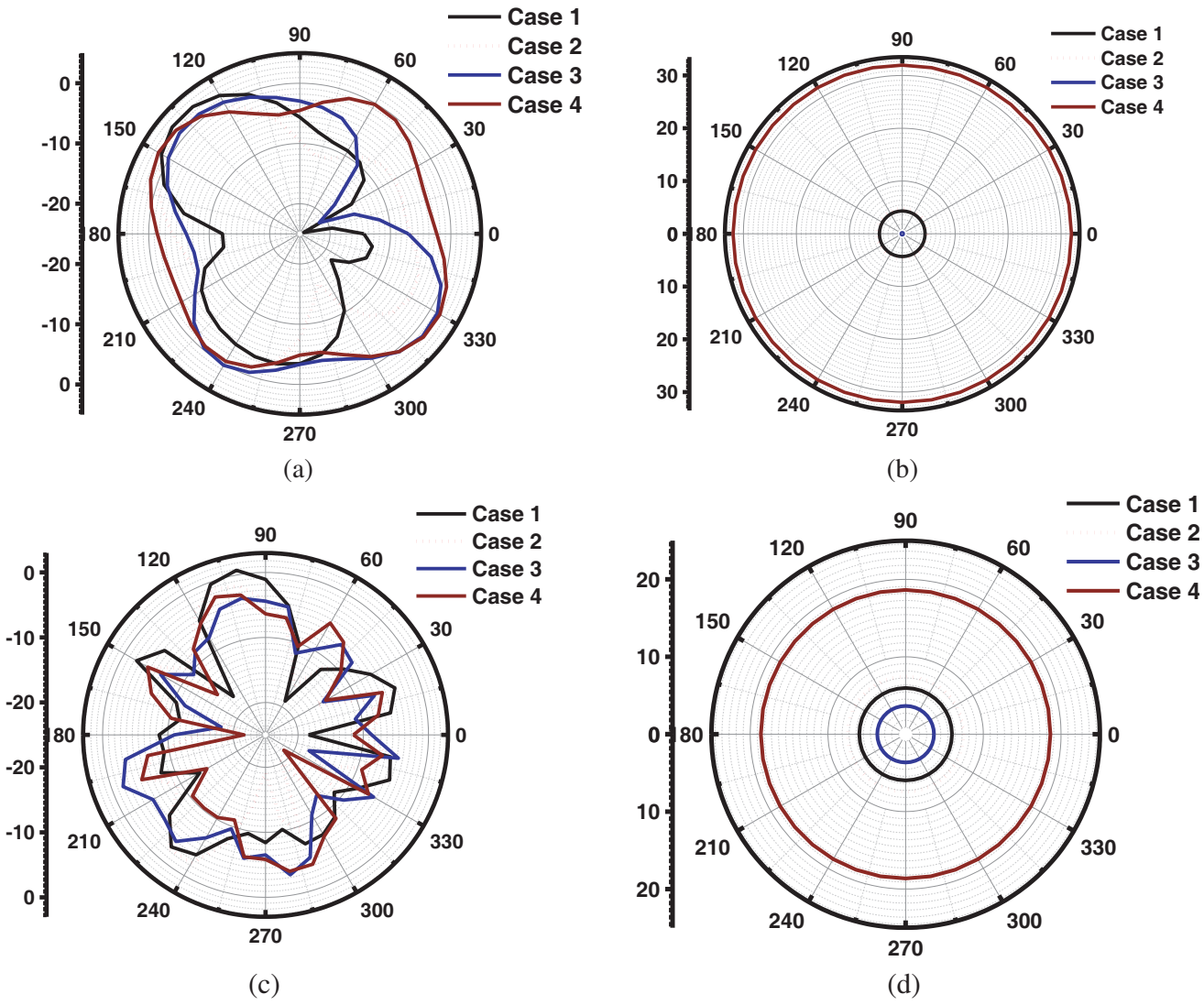

Figure 5. Simulated 2-D radiation patterns of 4×4 H-SRR MIMO antenna (design 2) for (a) H-plane at 2.4 GHz, (b) E-plane at 2.4 GHz, (c) H-plane at 5.2 GHz, and (d) E-plane at 5.2 GHz.

Table 3. Simulated gain, peak directivity, and beamwidth values of MIMO antenna at 2.4/5.2 GHz.

Cases	Frequency (GHz)	Gain (dB)	Peak directivity (dB)	Beamwidth (degrees)	Axial Ratio (dB)
1. Port 1 excited	2.4	4.32	5.13	47.55	11.84
	5.2	5.97	8.27	27.70	36.91
2. Port 1 and Port 3 excited	2.4	4.77	5.82	49.36	14.15
	5.2	7.44	8.57	31.37	30.24
3. Port 1, Port 2, and Port 3 excited	2.4	−0.21	3.78	46.91	26.19
	5.2	3.65	4.97	21.00	28.67
4. Port 1, Port 2, Port 3 and Port 4 excited	2.4	−31.96	1.83	53.99	26.14
	5.2	−18.64	5.15	28.05	28.18

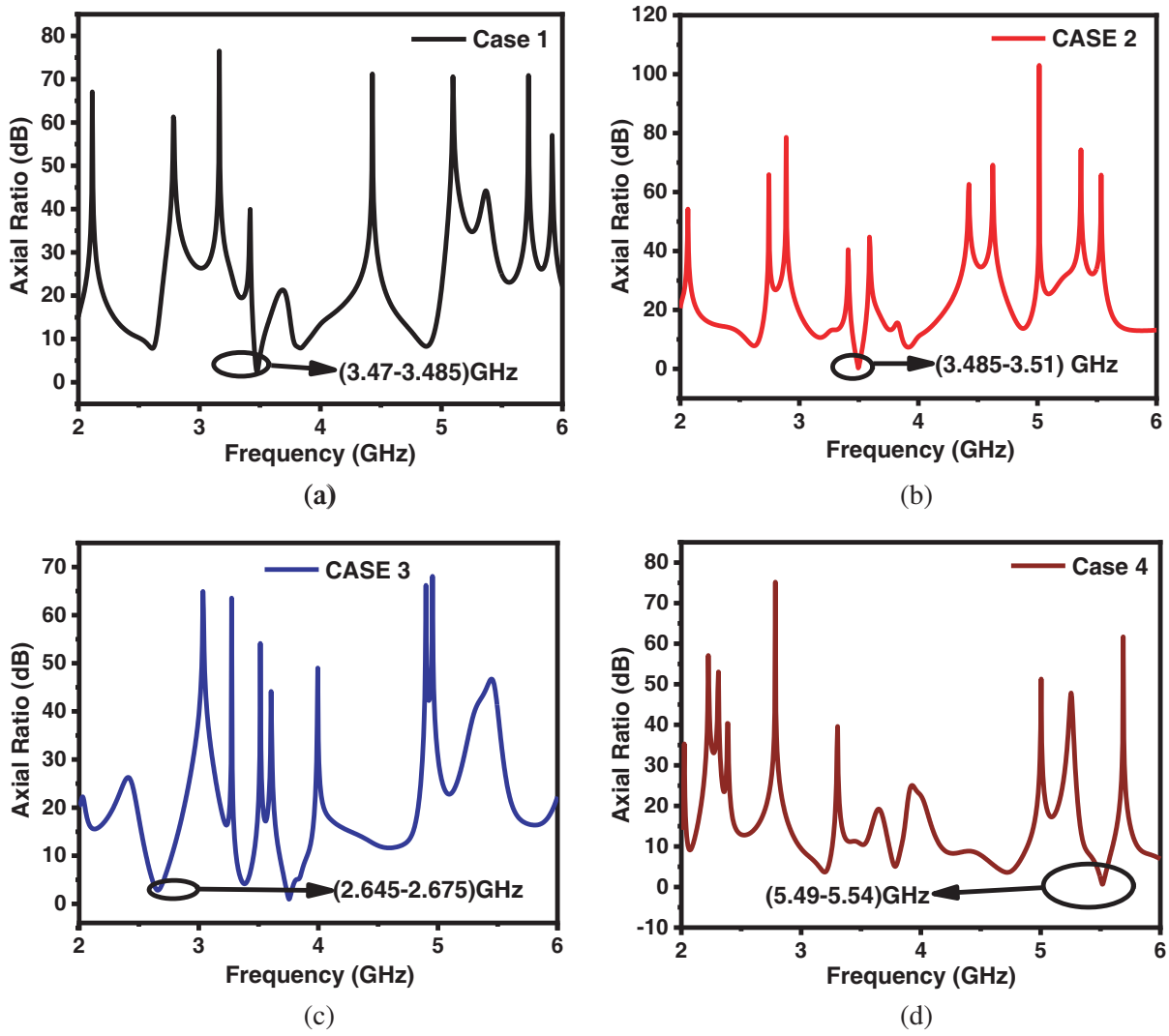

Figure 6. Axial ratio responses for (a) case 1, (b) case 2, (c) case 3, and (d) case 4.

Equation (1) [16].

$$ECC(\rho_{ij}) = \frac{\left|\iint_{4\pi} \bar{F}_i(\theta,\phi) \cdot \bar{F}_j^*(\theta,\phi)\, d\Omega\right|^2}{\iint_{4\pi} \left|\bar{F}_i(\theta,\phi)\right|^2 d\Omega \iint_{4\pi} \left|\bar{F}_j(\theta,\phi)\right|^2 d\Omega} \tag{1}$$

where the complex vectors, $\bar{F}_i(\theta,\phi)$ and $\bar{F}_j(\theta,\phi)$, denote the far-field radiation patterns of antenna i and antenna j, respectively, and $*$ denotes the Hermitian transpose of a matrix [16]. The ECC can also be obtained by using s-parameters of the MIMO antenna in Equation (2) [16],

$$ECC(\rho_{ij}) = \frac{\left|S_{ii}^* S_{ij} + S_{ji}^* S_{jj}\right|^2}{\left(1-|S_{ii}|^2-|S_{ij}|^2\right)\left(1-|S_{ji}|^2-|S_{jj}|^2\right)} \tag{2}$$

Figure 7(a) shows that ECC is found to be less than 0.04 in the frequency band of 2.4/5.2 GHz range, which is much below an acceptable value (< 0.5) for efficient working of a MIMO antenna [17], and hence the proposed MIMO antenna finds its usage for a range of dual-band frequency applications in WLAN/WiMAX systems [18]. Another parameter, TARC, is defined as the ratio of root square

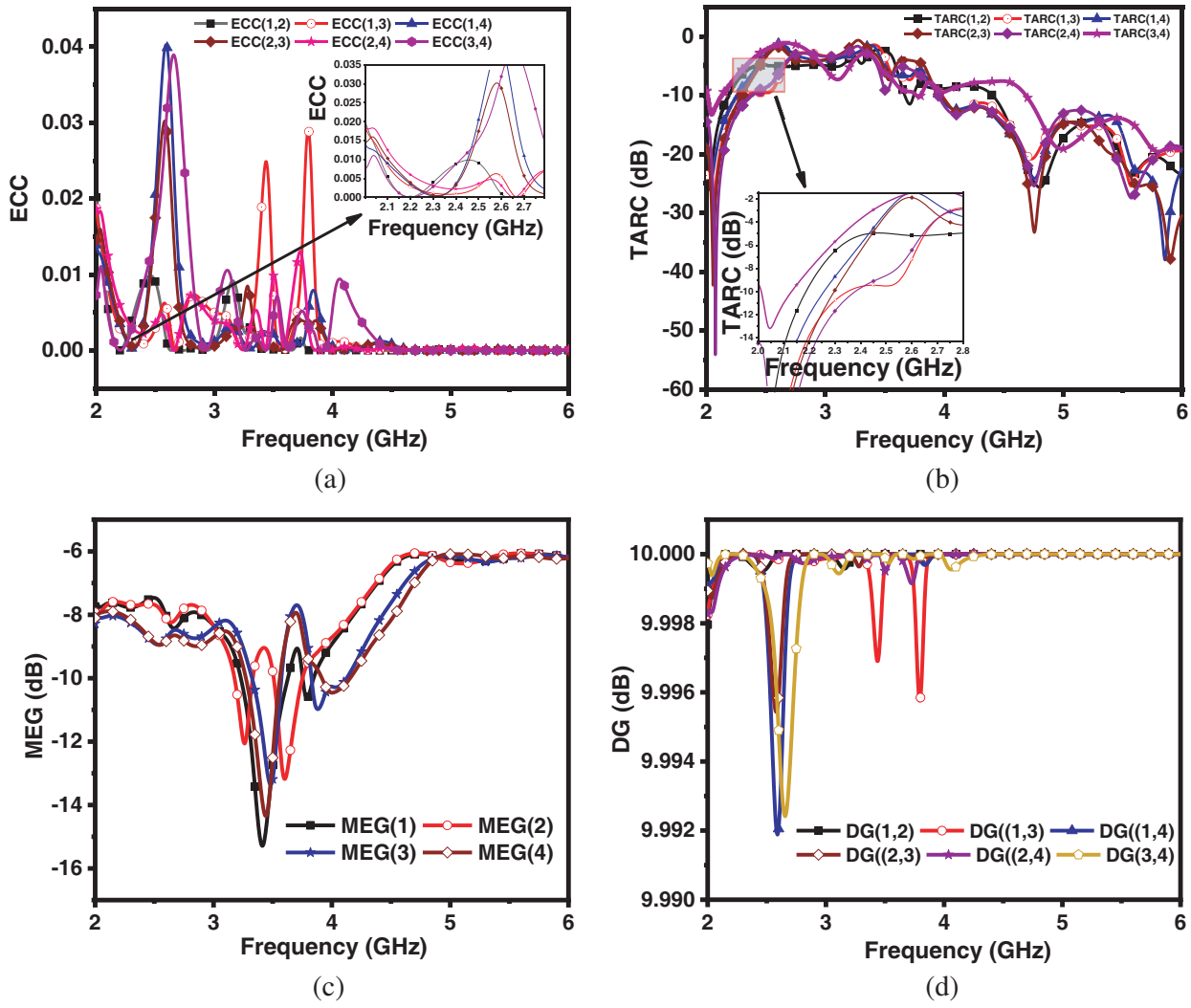

Figure 7. Simulated MIMO parameters performance of 4×4 H-SRR MIMO antenna for different port combinations, (a) ECC, (b) TARC, (c) MEG, and (d) DG.

total reflected power (b_i) to root square total incident power (a_i) by the antenna. For N-port MIMO antenna, it is defined as in Equation (3) [16]

$$TARC = \sqrt{\frac{\sum_{i=1}^{N} |b_i|^2}{\sum_{i=1}^{N} |a_i|^2}} \tag{3}$$

In terms of S-parameters for two ports, TARC is obtained using Equation (4) [19];

$$TARC = \sqrt{\frac{\left(S_{11}+S_{12}e^{j\theta}\right)^2+\left(S_{21}+S_{22}e^{j\theta}\right)^2}{2}} \tag{4}$$

where θ is the phase of associated S-parameter. Figure 7(b) shows the TARC plot with variation in the frequency range for different port combinations with TARC values in the range of -5 to -20 dB

at most frequencies in 2.4/5.2 GHz bands. Another important MIMO parameter, Mean Effective Gain (MEG) is defined as the ratio of average received power by a diversity antenna at a single port to the power received by an isotropic antenna in the operating band. It is desirable to have MEG value of less than 3 dB to ensure an equal power ratio to each antenna element [20]. For the N-port antenna system, MEG can be evaluated by [20],

$$MEG_k = 0.5\left(1 - \sum_{a=1}^{N} |S_{ka}|^2\right) \tag{5}$$

where N is the number of antennas. The simulated MEG values of the proposed MIMO antenna are shown in Figure 7(c), and MEG value is found to be $-8.48/-6.11$ dB at 2.4/5.2 GHz frequencies. Next, the diversity gain (DG) is obtained using Equation (6), which is defined as the amount of transmitted power that can be reduced without any loss in the diversity technique [19].

$$DG = 10\sqrt{1 - \left(ECC^2\right)} \tag{6}$$

In Figure 7(d), DG is found to be less than 10 dB in the entire band for the pairs of the ports of the proposed MIMO antenna. To check the loss in channel capacity of the proposed antenna due to the

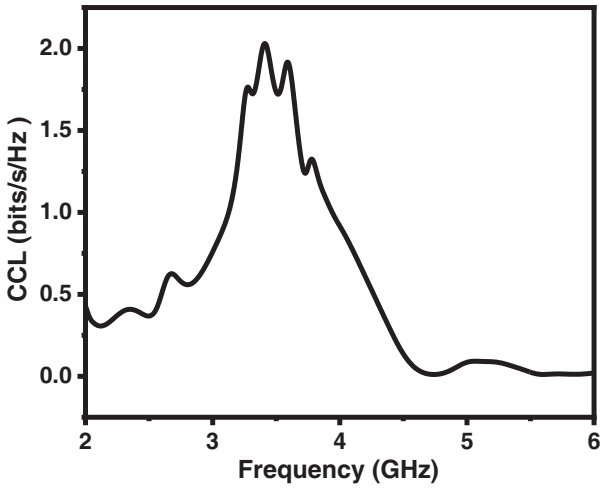

Figure 8. Channel capacity loss (CCL) response of the 4×4 H-SRR MIMO antenna.

Table 4. Comparison of present work with previously published literature.

Ref.	No. of Ports	Bandwidth (GHz)	ECC (max)	TARC	MEG	DG (dB)	CCL (bits/s/Hz) (min)
[4]	4	2.0–10.60	0.005	–	–	–	0.3
[9]	4	3.6–10.3	0.0022	better than −10 dB	–	> 9.9	0.3
[19]	4	3.1–10.6	0.4	better than −10 dB	< 1 dB	> 9.5	< 0.4
[21]	4	2.5–12.0	0.005	better than −6 dB	–	> 9.8	0.3
Present work	**4**	**2.0–6.0**	**< 0.04**	**better than −10 dB**	**−8.48 dB**	**< 10**	**0.09**

effect of correlation, CCL is calculated using Equation (7), which should be less than 0.4 bits per second per Hz for an N-port MIMO antenna [19, 21] as

$$CCL = -\log_2 \det(\mu_R) \tag{7}$$

where μ_R is the antenna correlation matrix [21]. The desirable value of CCL is < 0.4 bits per second per Hz, and as shown in Figure 8 it is 0.4/0.09 bits per second per Hz at 2.4/5.2 GHz frequencies. To show the novelty in the proposed MIMO design, a comparison with the previously published four-element UWB band MIMO antennas is shown in Table 4.

5. CONCLUSION

The 4×4 H-SRR MIMO antenna is presented for WLAN/WiMAX applications with pattern and polarization diversity. The measured return loss values of this antenna are found in close agreement with the simulated results at 2.4/5.2 GHz bands. The S-parameters are improved after placing the Z-structure between the HSRR antennas, and isolation is increased by about 30% in both bands as well as the impedance matching bandwidth by about 15%. Very low gain values even negative are obtained by exciting 3 or 4 ports of the proposed MIMO antenna while 1 or 2 port excitation gives positive gain up to a maximum about 6 dB. It is observed that the negative interference of multiple radiation patterns led to the negative gain, so the gain as well as directivity can be controlled on exciting various port combinations. The MIMO parameters like ECC, TARC, MEG, DG, and CCL are calculated to find the diversity performance of proposed MIMO antenna and are found in good agreement with the desired values for the WLAN/WiMAX communication purposes.

ACKNOWLEDGMENT

The authors would like to thank the Faculty Research Programme (FRP) of the Institute of Eminence (IoE) scheme of the University of Delhi (Letter ref. No. IoE/FRP/PCMS/2020/27 dated 31.12.2020).

REFERENCES

1. Clarke, R. N., "Expanding mobile wireless capacity: The challenges presented by technology and economics," *SSRN Journal*, Vol. 38, No. 8–9, 693–708, 2014.
2. Xu, H. and L. Yang, "Ultra-wideband technology: Yesterday, today, and tomorrow," *IEEE Radio and Wireless Symposium*, 715–718. 2008.
3. F.C.C., "FCC 1st report and order on ultrawideband technology," Washington, DC. Available: https://www.ieee802.org/802_tutorials/02-March/02133r1P802-15-WG_Ultra-Wideband-Tutorial.ppt.
4. Tripathi, S., A. Mohan, and S. Yadav, "A compact octagonal fractal UWB MIMO antenna with WLAN band-rejection," *Microwave and Optical Technology Letters*, Vol. 57, No. 8, 1919–1925, 2015.
5. Sipal, D., M. P. Abegaonkar, and S. K. Koul, "Easily extendable compact planar UWB MIMO antenna array," *IEEE Antennas and Wireless Propagation Letters*, Vol. 16, 2328–2331, 2017.
6. Bolin, T., A. Derneryd, G. Kristensson, V. Plicanic, and Z. Ying, "Two-antenna receive diversity performance in an indoor environment," *Electron. Lett.*, Vol. 41, 1205, 2005.
7. Chandel, R., A. K. Gautam, and K. Rambabu, "Design and packaging of an eye-shaped multiple-input-multiple-output antenna with high isolation for wireless UWB applications," *IEEE Transactions on Components, Packaging, and Manufacturing Technology*, Vol. 8, No. 4, 635–642, 2018.
8. Ben, I. M., L. Talbi, M. Nedil, and K. Hettak, "MIMO-UWB channel characterization within an underground mine gallery," *IEEE Trans. Antennas Propag.*, Vol. 60, 4874, 2012.
9. Kumar, A., "Compact 4×4 CPW-fed MIMO antenna with Wi-Fi and WLAN notch for UWB applications," *Radio Electronics and Communications Systems*, Vol. 64, No. 2, 92–98, 2021.

10. Zhang, S., Z. N. Ying, J. Xiong, and S. L. He, "Ultrawideband MIMO/diversity antennas with a tree-like structure to enhance wideband isolation," *IEEE Antennas Wireless Propag. Lett.*, Vol. 8, 1279, 2009.
11. Li, L., Z. L. Zhou, J. S. Hong, and B. Z. Wang, "Compact dual-band notched UWB planar monopole antenna with modified SRR," *Electron. Lett.*, Vol. 47, 950–951, 2011.
12. Sharma, Y., D. Sarkar, K. Saurav, and K. V. Srivastava, "Quad-band annular Z-structure and SRR based MIMO antenna system," 2015, doi: 10.1109/aemc.2015.7509143.
13. Peng, G., H. Shuang, W. Xubo, X. Ziqiang, W. Ning, and Z. Yi, "Compact printed UWB diversity Z-structure antenna with 5.5-GHz band-notched characteristics," *IEEE Antennas Wireless Propag. Lett.*, Vol. 13, 376–379, 2014.
14. Sengar, K., N. Rani, and A. Singhal, "Study and capacity evaluation of SISO, MISO, and MIMO RF Wireless Communication Systems," *International Journal of Engineering Trends and Technology (IJETT)*, Vol. 9, No. 9, 436–440, 2014.
15. Available: https://www.atlasrfidstore.com/rfid-insider/improve-rfid-read-range
16. Sharawi, M., "Printed MIMO antenna systems: Performance metrics, implementations, and challenges," *Forum for Electromagnetic Research Methods and Application Technologies (FERMAT)*, 1–11, 2014.
17. Available: https://www.antenna-theory.com/definitions/envelope-correlation-coefficient-ecc.php.
18. Pahadsingh, S. and Sahu, "Four-port MIMO integrated antenna system with DRA for cognitive radio platforms," *AEU International Journal of Electronics and Communications*, Vol. 92, 98–110, 2018.
19. Govindan, T., S. K. Palaniswamy, and M. Kanagasabai, "On the design and performance analysis of wristband MIMO diversity antenna for smart wearable communication applications," *Sci. Rep.*, Vol. 11, No. 21917, 2021.
20. Khan, A. A., M. H. Jamaluddin, S. Aqeel, J. Nasir, J. ur R. Kazim, and Owais, "Dual-band MIMO dielectric resonator antenna for WiMAX/WLAN applications," *IET Microwaves, Antennas & Propagation*, Vol. 11, No. 1, 113–120, 2017.
21. Sultan, K. S. and H. Abdullah, "Planar UWB MIMO-diversity antenna with dual notch characteristics," *Progress In Electromagnetics Research C*, Vol. 93, 119–29, 2019.
22. Varzakas, P., "Average channel capacity for rayleigh fading spread spectrum MIMO systems," *International Journal of Communication Systems*, Vol. 19, No. 10, 1081–1087, Dec. 2006.